

Mössbauer Study of the New Pyrochlore Form of FeF₃

Y. CALAGE,^{*,†} M. ZEMIRLI,^{*} J. M. GRENECHE,^{*} F. VARRET,^{*}
R. DE PAPE,[†] AND G. FERÉY[†]

^{*}Laboratoire de Spectrométrie Mössbauer, U.A. 807, and, [†]Laboratoire des Fluorures U.A. 449, Université du Maine, Route de Laval, 72017 Le Mans Cédex, France

Received July 16, 1986; in revised form October 16, 1986

Mössbauer spectrometry has been undertaken as a function of temperature on a new form of FeF₃ with the modified pyrochlore structure, recently synthesized by topotactic oxidation. The Mössbauer data (in zero field and in external magnetic field) lead to a noncollinear magnetic structure, in agreement with previous neutron diffraction results. The low value of T_N is discussed in terms of magnetic frustration. © 1987 Academic Press, Inc.

Introduction

Using a topotactic oxidation of the orthorhombic modified pyrochlore NH₄Fe₂F₆, a new form of FeF₃ (Pyr. FeF₃), with the cubic pyrochlore structure, was synthesized (1).

The cubic cell ($Fd\bar{3}m$, $a = 10.325(2)$ and $10.292(8)$ Å respectively at 300 and 4.2 K) contains 16 formula units. The antiferromagnetic structure of Pyr. FeF₃ ($T_N = 20(2)$ K) is described by four ferromagnetic sublattices at 109° to each other (2).

This paper deals with the Mössbauer data of Pyr. FeF₃. The other forms of FeF₃, rhombohedral (3), hexagonal tungsten bronze (H.T.B.) (4), and amorphous (5), were previously analyzed by Mössbauer spectroscopy. Their magnetic properties are strongly dependent on the topology of the cationic subnetwork (magnetic ordering temperatures range from 363 to 36 K).

Experimental

Powder samples of different syntheses have been prepared, containing 5 mg Fe cm⁻², for Mössbauer experiments out of field and under external magnetic field.

Mössbauer spectra have been recorded over the temperature range 2–300 K on a spectrometer driven with a triangular velocity signal, using a ⁵⁷Co source diffused into a rhodium matrix. The hyperfine data were refined with the MOSFIT program for the study as a function of temperature and with the MOSHEX program for the study under external magnetic field (6).

Results and Discussion

(a) Quadrupole and Magnetic Data

All the samples studied contained at least two Fe³⁺ components and a small Fe²⁺

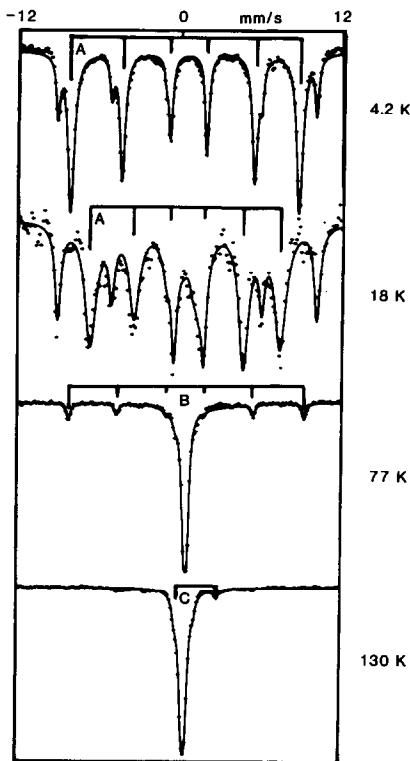


FIG. 1. Mössbauer spectra obtained at various temperatures, for phase identification. (A) Pyr. FeF₃ is magnetically split at 18 K, (B) H.T.B. FeF₃ is starting to split at 130 K, and (C) Fe²⁺ splits between the spectra at 77–130 K. Also notice the small asymmetry of the magnetic lines at 4.2 K.

component. Mössbauer spectra at several temperatures are shown in Figs. 1 and 2; fitted data listed in Table I allow one to characterize H.T.B. FeF₃ as a major impurity according to data of Ref. (4). Fe²⁺ splits

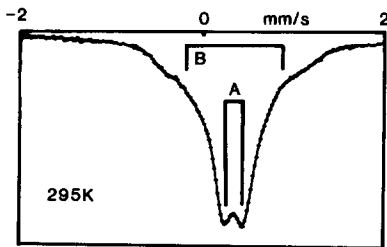


FIG. 2. Paramagnetic Mössbauer spectrum at 295 K showing (A) Pyr. FeF₃ and (B) H.T.B. FeF₃.

TABLE I
PHASE CHARACTERIZATION FROM MÖSSBAUER SPECTRA

| T (K) | V (mm/s) | Pyrochlore FeF ₃ | | | | Hexagonal tungsten bronze FeF ₃ | | | | Fe ²⁺ | | | | | |
|-------|----------|-----------------------------|----------|----------------|------------------------|--|--------------------------|----------|----------|------------------------|----------------|----------------|----------|------------------------|---|
| | | I.S. ^a (mm/s) | Γ (mm/s) | Δ or 2δ (mm/s) | H _{hyp} (kOe) | % | I.S. ^a (mm/s) | Γ (mm/s) | Δ (mm/s) | H _{hyp} (kOe) | % | Γ (mm/s) | Δ (mm/s) | H _{hyp} (kOe) | % |
| 295 | ± 2 | 0.48 | 0.34 | 0.24 | — | 76 | 0.46 | 0.76 | — | 15 | 1.25 | 0.32 | 2.76 | — | 9 |
| 130 | ± 12 | 0.56 | 0.40 | 0.24 | — | 76 | 0.58 | 0.76 | — | 17 | 1.35 | 0.24 | 2.98 | — | 7 |
| 120 | ± 12 | 0.58 | 0.52 | 0.25 | — | 79 | 0.56 | 0.11 | 418 | 17 | 1.43 | 0.24 | 3.05 | — | 4 |
| 100 | ± 12 | 0.58 | 0.50 | 0.25 | — | 77 | 0.57 | 0.46 | 494 | 19 | 1.42 | 0.24 | 3.08 | — | 4 |
| 77 | ± 12 | 0.59 | 0.40 | 0.24 | — | 80 | 0.58 | 0.11 | 532 | 20 | — ^b | — ^b | — | — | — |
| 4.2 | ± 12 | 0.58 | 0.46 | -0.22 | 517 | 79 | 0.60 | 0.07 | 586 | 21 | — ^b | — ^b | — | — | — |

^a The isomer shift (I.S.) values are relative to metallic iron at room temperature.
^b This component was not taken into account during the fitting procedure.

magnetically between 130 and 77 K spectra and therefore is likely to be in the rutile FeF₂ form, probably far from structural perfection since the corresponding magnetic lines (7) could not be fitted.

The hyperfine data of the pyrochlore FeF₃ phase are presented in Table II. The thermal variation of the magnetic hyperfine field is shown in Fig. 3; the magnetic ordering temperature $T_N = 21.8(5)$ K was established by thermal scanning (Fig. 4).

The inhomogeneous broadening of the magnetic lines of Pyr. FeF₃ is of special interest. It becomes larger and larger as T_N is approached from below. On the other hand, the paramagnetic lines do not show any sizeable broadening above T_N (this is also reflected by the flat part of the thermal scan above 22.5 K in Fig. 4). This behavior does not give evidence for critical spin fluctuations around T_N , but rather suggests molecular field distribution due to some departure from structural perfection (and also responsible for the asymmetrical lineshape of the magnetic lines at 4.2 K).

In the pyrochlore structure (*Fd3m*), the electric field gradient is axial along the (111) axis (8). Therefore, the shift of the two outermost magnetic lines due to quadrupole interaction is given by

$$\varepsilon = (eQV_{zz}/8)(3 \cos^2\theta - 1),$$

where θ is the angle between the principal

TABLE II
HYPERFINE DATA OF THE PYROCHLORE FeF₃

| T (K) | V (mm/s) | I.S. ^a (mm/s) | Δ or $2e$ (mm/s) | H_{hyp} (kOe) | Γ (mm/s) |
|------------|---------------|-----------------------------|----------------------------|---------------------------|----------------------------------|
| 295 | ± 2 | 0.48(2) | 0.24(2) | — | 0.34(2) |
| 77 | ± 2 | 0.58(2) | 0.24(2) | — | 0.31(2) |
| 20 | ± 12 | 0.58(2) | -0.27(4) | 366(5) | 0.70(5) |
| 15 | ± 12 | 0.59(2) | -0.26(4) | 473(4) | 0.60, 0.92, 1.00(4) ^b |
| 10 | ± 12 | 0.57(2) | -0.21(3) | 503(3) | 0.66, 0.88, 1.10(4) ^b |
| 4.2 | ± 12 | 0.58(1) | -0.22(2) | 517(2) | 0.37, 0.48, 0.57(2) ^b |
| 2 | ± 12 | 0.58(1) | -0.21(2) | 519(2) | 0.38, 0.51, 0.62(2) ^b |

^a The isomer shift (I.S.) values are relative to metallic iron at room temperature.

^b Fit using three independent values for lines 3-4, 2-5, and 1-6, respectively.

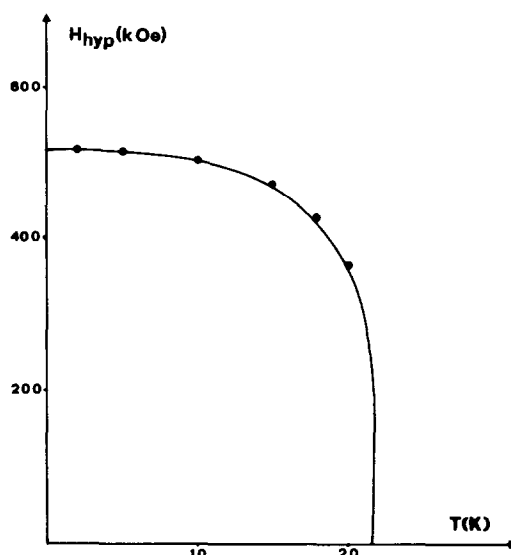


FIG. 3. Thermal variation of the hyperfine field H_{hyp} for Pyr. FeF₃.

axis V_{zz} of the electric field gradient (EFG) tensor and the hyperfine field. This quadrupolar shift ε can be compared to the quadrupolar splitting Δ given by

$$\Delta = |eQV_{zz}/2|.$$

The data are consistent with a negative

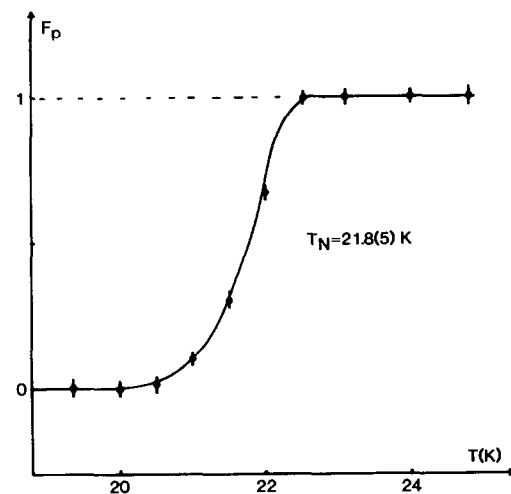


FIG. 4. Thermal variation of the paramagnetic fraction F_p of Pyr. FeF₃ ($V_{\text{scan}} = \pm 0.40$ mm/s).

main component V_{zz} and an angle θ close to zero.

A point charge model calculation (monopolar and dipolar contributions) was undertaken to calculate the EFG. The principal axis V_{zz} lies in the (111) direction of the cubic cell and the total EFG gives a small and negative V_{zz} (-0.6 mm/s) in qualitative agreement with the Mössbauer results. A quantitative agreement would require a fluorine polarizability of $0.5\text{--}0.6 \text{ \AA}^3$, which is lower than the usual values ($\approx 1.0 \text{ \AA}^3$) (7). The small disagreement might be due to covalency effects which are not accounted for, or to inaccuracies in atomic positions and Mössbauer data.

(b) Mössbauer Study under Magnetic Field

Spectra shown in Fig. 5 were recorded at 4.2 K under 0, 4, and 7 tesla, the field being parallel to the γ -beam direction.

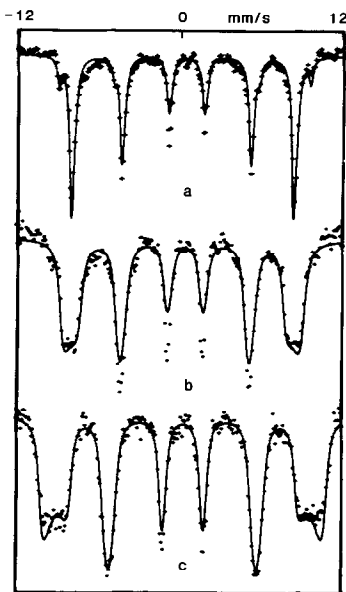


FIG. 5. Mössbauer spectra of Pyr. FeF_3 at 4.2 K at field (a) 0 kOe, (b) 40 kOe, and (c) 70 kOe. Spectra (b) and (c) have been fitted using a speromagnetic model (5) to describe a random powder with a magnetic structure unaffected by the external field. The second magnetic component was not resolved in (b) and (c).

According to the literature (for instance, Ref. (9, Fig. 3d)), the shape of these spectra is characteristic of a random powder with a magnetic structure which is not oriented by the external field. This shape is quite similar to that of amorphous FeF_3 , a textbook example for speromagnetism (5); so, the speromagnetic model (6) was used to fit the spectra. However, the magnetic structure of Pyr. FeF_3 cannot be speromagnetic in the absence of topological disorder. The lack of orientation under external magnetic field may be due to a complex noncollinear magnetic structure with antiferromagnetic sublattices (similar to that of ZnFe_2O_4 (10)); this is consistent with magnetic moments parallel to the local gradient axes (i.e., along the four (111) directions).

These results also agree with a previous neutron diffraction study which revealed four ferromagnetic sublattices at 109° from each other (2).

An alternative explanation for the lack of orientation under external field, based on a large anisotropy energy, seems less probable since another ferric fluoride with comparable T_N such as $\beta\text{-FeF}_3 \cdot 3(\text{H}_2\text{O})$ (11) presents spin rotation under external magnetic field of comparable magnitude.

In any case, the spectra were fitted using the speromagnetic model previously described. The extra contribution of H.T.B. FeF_3 could not be taken into account because this form has not yet been studied under external field. The fitted data, reported in Table III, show a weak discrepancy from the ideal speromagnetic model in the H_{hyp} values which are expected to be constant.

(c) Comparison with Other Forms of FeF_3

All hyperfine data obtained on the different forms of FeF_3 , crystalline and amorphous, are listed in Table IV.

Isomer shift values are very similar, typical of Fe^{3+} with sixfold F^- coordination.

In all forms of FeF_3 , the interactions are

TABLE III
HYPERFINE DATA OF MÖSSBAUER SPECTRA
OBTAINED UNDER EXTERNAL MAGNETIC FIELD^a

| kG | I.S. ^b (mm/s) | Γ (mm/s) | 2ε (mm/s) | H _{hyp} (kOe) |
|----|-----------------------------|-------------|--------------------|---------------------------|
| 0 | 0.58(1) | 0.46(2) | -0.23(1) | 517(3) |
| 40 | 0.60(3) | 0.48(3) | -0.23 ^c | 515(3) ^d |
| 70 | 0.61(3) | 0.66(4) | -0.23 ^c | 495(5) ^d |

^a Parallel to the γ-beam, fitted using a speromagnetic model (5).

^b The isomer shift (I.S.) values are relative to metallic iron at room temperature.

^c This value is fixed during the fitting procedure.

^d H_{hyp} is assumed parallel to the EFG axis.

mainly antiferromagnetic between nearest Fe³⁺ neighbors. As previously noted (2), the evolution of the hyperfine field values can be correlated to the variation of the Fe-F superexchange angle in the different structures: H_{hyp} decreases linearly with cos² θ. The drastic decrease of T_N, with respect to the other crystalline forms of FeF₃, may be interpreted in terms of magnetic frustration (2); it follows the percent-

TABLE IV
HYPERFINE DATA ON THE CRYSTALLINE AND
AMORPHOUS FORMS OF FeF₃

| | I.S. ^a (mm/s) | H _{hyp} ^b (kOe) | T _N ^c (K) | Δ ^d (mm/s) | Reference |
|---------------------------------------|-----------------------------|--|------------------------------------|--------------------------|-----------|
| Rhombohedral | 0.49 | 618 | 363 | ≈0.0 | (3) |
| Hexagonal | 0.47 | 577 | 105 | ≈-0.20 | (4) |
| Hexagonal, hydrated | 0.44 | 560 | 129 | 0.66 ^f | (4) |
| Pyrochlore | 0.48 | 517 | 22 | -0.22 | This work |
| Amorphous, evaporated ^e | 0.46 | 560 | 39 | 0.58 ^g | (5) |
| FeF ₃ · xHF ^e | 0.48 | 560 | 36 | 0.56 ^g | (12) |

^a Isomer shift values relative to metallic iron at room temperature.

^b Hyperfine field values obtained at 4.2 K.

^c Magnetic ordering temperature established by thermal scanning.

^d Quadrupolar interaction values in the paramagnetic phase.

^e Average values for I.S., H_{hyp}, and Δ.

^f No sign determined.

^g Both signs with equal probabilities.

age of frustrated bonds (i.e., bonds involved in triangular cycles of the magnetic network). This percentage is maximum with the pyrochlore structure in which Fe³⁺ forms a tetrahedral magnetic network. From this point of view, amorphous FeF₃, despite the absence of long-range order, seems less frustrated than Pyr. FeF₃ (Table IV). Its magnetic situation is in between those of Pyr. and H.T.B. FeF₃ and should be analyzed in terms of superexchange angle distributions and ring statistics in the structure.

Acknowledgment

The authors gratefully acknowledge Mrs. Duroy (CNRS Le Mans) for her help during the preparation of the samples.

References

1. R. DE PAPE AND G. FERREY, *Mater. Res. Bull.* **21**, 971 (1986).
2. G. FERREY, R. DE PAPE, M. LEBLANC, AND J. PANNETIER, *Rev. Chim. Minel.*, **23**, 474 (1986).
3. G. K. WERTHEIM, H. J. GUGGENHEIM, AND D. N. E. BUCHANAN, *Phys. Rev.* **169**, 465 (1968).
4. Y. CALAGE, M. LEBLANC, G. FERREY, AND F. VARRET, *J. Magn. Magn. Mater.* **43**, 195 (1984).
5. G. FERREY, F. VARRET, AND J. M. D. COEY, *J. Phys. C* **12**, L531 (1979).
6. J. TEILLET AND F. VARRET, unpublished programs MOSFIT and MOSHEX.
7. G. K. WERTHEIM AND D. N. E. BUCHANAN, *Phys. Rev.* **161**, 478 (1967).
8. Y. CALAGE AND J. PANNETIER, *J. Phys. Chem. Solids* **38**, 711 (1977).
9. J. CHAPPERT, J. TEILLET, AND F. VARRET, *J. Magn. Magn. Mater.* **11**, 100 (1979).
10. V. BECKMANN, G. RITTER, H. SPIERING, AND H. WEGENER, in "Proceedings, Conference on the Application of the Mössbauer Effect, Tihany, 1969."
11. P. IMBERT, Y. MACHETEAU, AND F. VARRET, *J. Phys. (Orsay. Fr.)* **34**, 49 (1973).
12. J. M. GRENECHE, M. LEBLANC, F. VARRET, AND G. FERREY, *Hyp. Int.* **27**, 317 (1986).
13. J. M. GRENECHE, F. VARRET, M. LEBLANC AND G. FERREY, *Sol. State Comm.*, in press.